

Classification of Al-Chabaish Marshes Satellite Images in Iraq using Support Vector Machine Technique

Saad M. Hel¹, Bushra Q. Al-Abudi²

Department of Astronomy and Space, College of Science, University of Baghdad, Baghdad, Iraq

Abstract: *In this paper, Landsat satellite images of AL-Chabaish marshes and surrounding district in (DhiQar) province in the south of Iraq are classified for years 1990, 2000, 2015 and 2017 using two software programming these are: MATLAB r2017a 2017 and ENVI 5.3 2017. Principle components analysis (PCA) is applied on six bands of these satellite images using MATLAB and the information of all six bands concentrated in first three principle components and then blended to form integrated image. Then the integrated image is partitioned using Adaptive Horizontal-Vertical partitioning scheme, finally supervised Support Vectors Machine (SVM) technique is applied to classify the image. While supervised method (Maximum likelihood) using ENVI software is utilizing to compare the results. The results from using SVM provided high accuracy these are, 90.98%, 93.21%, 92.17% and 91.13% for years 1990, 2000, 2015 and 2017 respectively. The results indicated that the AL-Chabaish marshes from 1990 to 2017 are suffering many artificially and naturally change, this clearly impact in the Landover. In 1990 the marshes drying and this causes reduce in a vegetation, water and increase in openland, shallow water, the effect of drying it was very clear in 2000, 2015, and 2017 the AL-Chabaishl and cover situation improved much as the amount of water and vegetation increased with a decreasing in the openland*

Keywords: Support Vectors Machine, Landsat satellite images, Principle components analysis, AL-Chabaish Marshes

1. Introduction

Remote sensing provides images of areas in a fast and cost-efficient manner, and attempts to demonstrate the "what is happening right now" in a study area. Also remote sensing techniques give quick methods to detect the environmental changes, such that change detection is an important application of remote sensing in environmental. Change detection is a process of identifying differences in the state of objects or phenomena by observing them at different time (multi-temporal analysis) [1], therefore change detection became useful tool for detecting land cover changes. It has enabled to observe changes over large areas and provided long-term monitoring capabilities. In general digital change detection techniques using temporal remote sensing data are useful to help analyze. These data, and provided detailed information for detecting change in land cover [2]. The area under study is Al-Chabaish marshes that considerable one of the distant areas. One of the main purposes of satellite remote sensing is to interpret the observed data and classify features. In addition to the approach of photo interpretation, quantitative analysis, which uses computer to label each pixel to particular spectral classes (called classification), is commonly used. Quantitative analysis can perform true multispectral analysis, make use of all the available brightness levels and obtain high quantitative accuracy. [3]. The two general classification methods which are used most often are: supervised and unsupervised classification, The main difference between the two methods is that the classification observer built on real information about geographical phenomena given the current computer, while the rating unattended done in accordance with mathematical equations define gatherings clusters and thus classification categories, according to the relationship between the numeric values of the ranges of image [4]. Mechat N., et.al [5] Used Support vector machines (SVM) to classify plane targets on a binary remote sensing. The experimental results

show that support vector machines can generalize well on difficult image classification problems where the only features are high dimensional binary values. Moreover, they observed that the range of the binary values of images affect the performance of classification results. Ratna D., et. al. [6] Used support vector machines for defect detection and classification of bullets image. The Principal Component Analysis (PCA) applied and Performance of the proposed classification of bullets image was tested using 80 images of bullets in which 40 images free of defects and 40 images with defect. The results show that the (SVM) can classify images of bullets with a 90% accuracy rate.

2. Study Area

The central marshes are located in southeastern Iraq and are common to the three governorates of Maysan, DhiQar and Basra. The average length of the mountain is about 2.75 meters, and the maximum extension of the mountains in recent years after the re-dredging about 1176 square kilometers with a height of 1.9 meters. The central marshes are characterized by a number of deep ponds such as the Baghdad pond. The central marshland environment is characterized by its biological diversity as it is home to many Species of reed and papyrus, as well as birds and fish. It is a migratory and endangered bird plant. The negative effects of the phenomenon of desertification and climate change and improving the environmental reality of the region. UNESCO voted to include the marshes as a world heritage in 2016. The marshes today became one of the tourist attractions in Iraq [7]. Al-Chabaish Marshes is one of the large marshes in the south of Iraq, it is comprised a vast complex of mostly permanent freshwater marshes, with scattered areas of open water, located to the west of the Tigris river and north of the Euphrates river (within Basra, DhiQar, and Missan provinces). Covering an area of (3000 km²), it is bounded by the longitudes 46° 47' to 47° 21' E

and Latitude 30° 55' to 31° 23' N and represent many diverse habitats from seasonal to permanent marshes. Figure 1 shows the original map of Iraq and the image inside the square form represents study area [7].



Figure 1: The study area on the map of Iraq in 2017

3. Proposed Classification Methods

Different methods of classification were used and analysed these can be summarized in the block diagram in figure 2 .More details of each step in this block diagram will be explain in the following sections

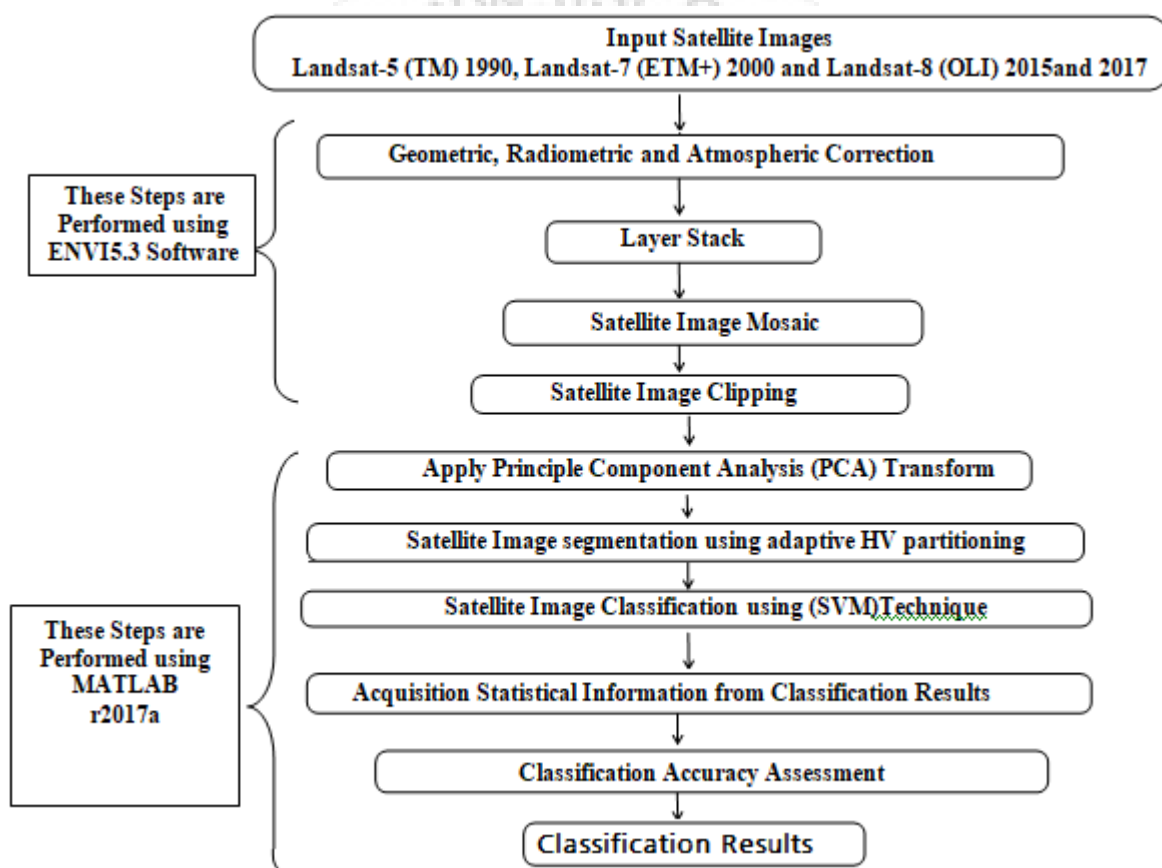


Figure 2: Block Diagram of the proposed classification method

3.1 Applying Principle Component Analysis

Principal Component Analysis (PCA) is a dimension-reduction tool that can be used to reduce a large set of variables to a small set that still contains most of the information in the large set. Principal component analysis (PCA) is a mathematical procedure that transforms a number of (possibly) correlated variables into a (smaller) number of uncorrelated variables called principal components analysis (PCA). In this section, we performed PCA on all six bands (1, 2, 3, 4, 5, 6) of AL-Chabaish marshes satellite images for

years (1990 and 2000) and six bands (2, 3, 4, 5, 6, 7) for years (2015 and 2017). The six bands yield six principle components, the first (PC) has most information's of the six bands, this information gradually decreasing in the other (PCs). In this work, we blended first three components (PC1, PC2, PC3) with different ratio depending on variance of (PC). By calculating the variance for each first three (PCs) and then divided it by the total number of variance, we get the following ratio:

$$PC = 0.81 PC1 + 0.14 PC2 + 0.05 PC3 \dots\dots\dots (1)$$

Figure 3 shows the resulted first three component images with different ratio for years 1990, 2000, 2015 and 2017, while, figure 4 shows the first three component color's images for years 1990, 2000, 2015 and 2017.

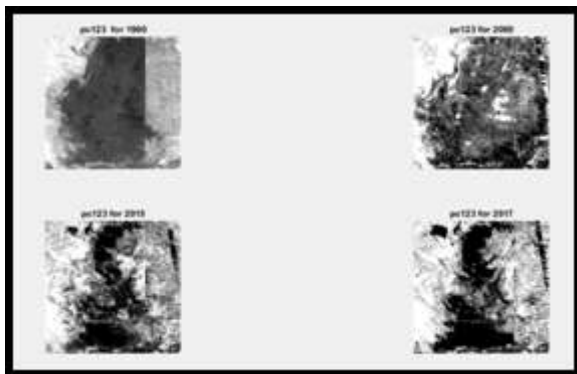


Figure 3: the first three components (PCs) images for years (1990, 2000, 2015 and 2017).

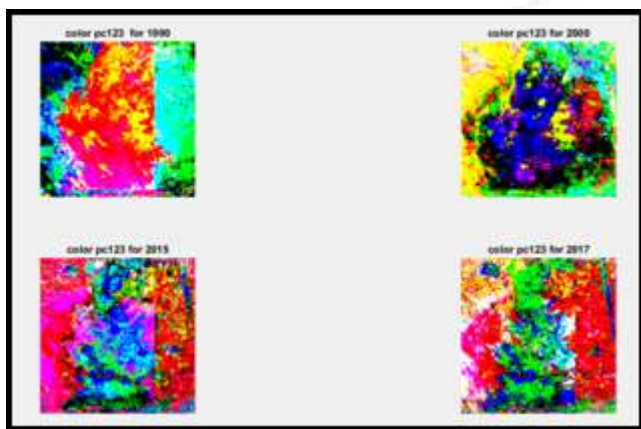


Figure 4: The first three components (PCs) image color's for years (1990, 2000, 2015 and 2017).

3.2 Satellite Images Segmentation

In this section we applied the adaptive HV partitioning method on the resulted first three components images from applying PCA. The adaptive HV partitioning is based on computing the directional difference between the mean values of top-bottom and left-right halves of the blocks, i.e.,

$$d_H = \left| \sum_{i=0}^{H-1} \left[\sum_{j=0}^{\frac{W}{2}-1} f_{i,j} - \sum_{j=\frac{W}{2}}^{W-1} f_{i,j} \right] \right| \quad (2)$$

$$d_V = \left| \sum_{j=0}^{W-1} \left[\sum_{i=0}^{\frac{H}{2}-1} f_{i,j} - \sum_{i=\frac{H}{2}}^{H-1} f_{i,j} \right] \right| \quad (3)$$

Where, $f_{i,j}$ is the pixel values at the position (i, j), W is the block width, H is the block height, d_H is the horizontal difference, d_V is the vertical difference. Then the larger difference is checked, if d_H is the largest and it is bigger than a threshold value then a horizontal partitioning decision will be taken. While, if d_V is the largest and bigger than a threshold value then a vertical partitioning decision will be taken, otherwise no partitioning is performed on the block. In this paper, an adaptation will be used to improve the

mechanism of the HV partitioning process by implementing the quadtree partitioning on each block which isn't satisfy the uniformity criterion of HV partitioning, therefore, we used the partitioning control parameters that are implemented in quadtree partitioning (i.e., inclusion factor and acceptance ratio). This hybrid partitioning method will be referred as an adaptive HV partitioning and it is expected to improve the efficiency of the HV partitioning. The implementation of the adaptive HV partitioning method can be demonstrated as follows:

- 1) Compute the global mean (M) and standard deviation (σ) of the whole input image,
- 2) Inclusion factor (α): represent the multiple factor, when it is multiplied by the global standard deviation (σ) it will define the value of the extended standard deviation (σ_e), i.e. $\sigma_e = \alpha\sigma$.
- 3) Set the values of the partitioning control parameters (i.e., maximum block size, minimum block size, inclusion factor, and acceptance ratio). In addition to these parameters, another parameter was used to control the partitioning process, it is called the "Mean factor (m.)", this parameter represents the multiplication factor, when it is multiplied by the global mean (M) it will define the value of the extended mean (M_e), i.e., $M_e = mM$
- 4) The HV partitioning information is stored by utilizing the HVLinkList, which is looks like the QuadtreeLinkList used in the quadtree partitioning, it is consist of the same parameters except the size parameter, since the HV partitioning based on rectangles (i.e., width not equal to height), thus we need to assign both dimensions of each block. The designed HVLinkList consists of the followings:
 - a) Position: represented by the X and Y coordinates of the top-left corner of the image block
 - b) X Size: represent the width of the image block.
 - c) Y Size: represent the height of the image block.
 - d) Next: represent a pointer to the next block. Initialize the first LinkList record with the following element values:-
 With LList (0)
 X= 0
 Y= 0
 XSize = W
 YSize = H
 Next = Nil
 end with
- 5) For each sub-block, check the directional uniformity criterion that is used as a measure to decide whether the sub-block will be partitioned into halves or not, and in which direction the partitioning will be performed. The directional uniformity criterion was implemented by applying the following steps: -
 - a) Subdivide each subblock into four quarters and determine the mean values for each quarter (M_{LT} ,

M_{RT} , M_{LB} , and M_{RB}), the labels LT, RT, LB, and RB represent the mean values of the left-top, right-top, left-bottom, and right-bottom quarters, respectively.

- b) Calculate the mean values of the left half (M_L) right half (M_R), top half (M_T), and bottom half (M_B), then, determine the horizontal and vertical differences as follows:

$$d_H = |M_L - M_R|$$

$$d_V = |M_T - M_B|$$

- c) Determine the index (I) as follows:-

$$I = \begin{cases} 3 & \text{if } d_H \geq d_V \text{ and } d_H > M_e \text{ and } W > S_{\min} \\ 2 & \text{if } d_V \geq d_H \text{ and } d_V > M_e \text{ and } H > S_{\min} \\ 1 & \text{if } N_P / S > R \\ 0 & \text{otherwise} \end{cases}$$

Where, W is the block width (i.e., Xsize), H is the block height (Ysize), S_{\min} is the minimum allowable block size. The value of index (I) will be the value (3) when a horizontal partitioning decision was taken, the value (2) means a vertical partitioning decision was taken, while the value (1) means quadtree partitioning decision was taken, and finally the value (0) means don't partition. The partitioning processes will continue until the rectangular sub-blocks cannot further divided.

3.3 Satellite Image Classification using (SVM) Algorithm

Support Vector Machines (SVMs) are a relatively new supervised classification technique to the land cover mapping community. They have their roots in Statistical Learning Theory and have gained prominence because they are robust, accurate and are effective even when using a small training sample. By their nature SVMs are essentially binary classifiers, however, they can be adopted to handle the multiple classification tasks common in remote sensing studies. In this section we applied SVM algorithm[8] on the resulted satellite images from adaptive HV partitioning method as the classification results from applying SVM technique can be shown in figures (5-8) of AL-Chabaish marshes satellite images for years 1990, 2000, 2015 and 2017 respectively, while, tables (1-4) presentation the statistical results of classification for year 1990, 2000, 2015 and 2017 respectively. Table (5) illustrated the change in years 2000, 2015 and 2017 comparing with year 1990. The results indicated that five classes found with comparison with the original image. These classes represent five major features in the study area (water, vegetation, alluvial soil, shallow water and openland).

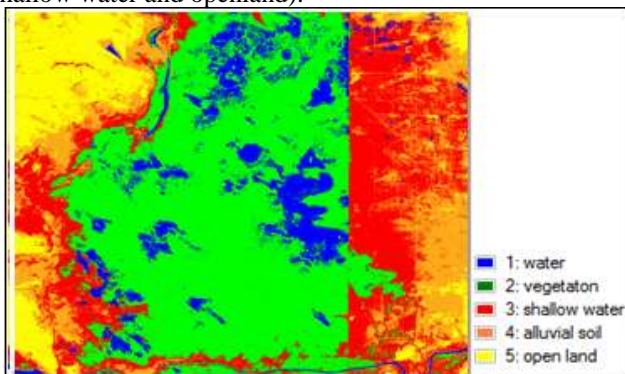


Figure 5: Classification results of supervised SVM technique for AL-Chabaish satellite image for year 1990

Table 1: Statistical results of supervised SVM Classification for AL-Chabaish Satellite Image for year 1990

Class No.	Class Name Landsat-5 (TM) (1990)	Class Color	Class Area (m ²)	Class Area (km ²)	Percent (%)
1	Water	Blue	263457013.5	263.4570135	9.228688
2	Vegetation	Green	1239137090	1239.13709	43.405979
3	Shallow water	Red	620889286.2	620.8892862	21.749254
4	Alluvial soil	Magenta	427441496.8	427.4414968	14.972933
5	Open Land	Yellow	303836413.1	303.8364131	10.643146
	Total		2854761300	2854.7613	100

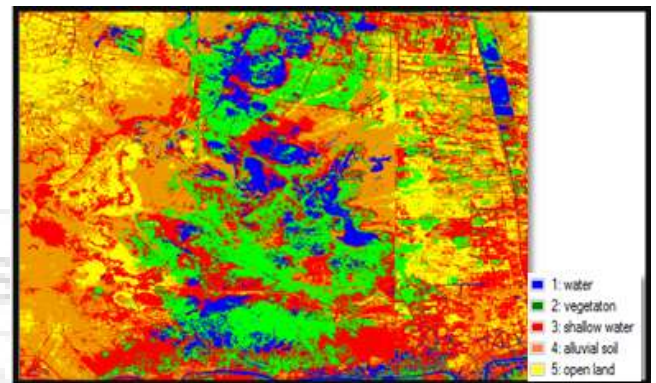


Figure 6: Classification results of supervised SVM technique for AL-Chabaish satellite image for year 2000.

Table 2: Statistical results of supervised SVM Classification for AL-Chabaish Satellite Image for year 2000

Class No.	Class Name Landsat-7 (ETM+) (2000)	Class Color	Class Area (m ²)	Class Area (km ²)	Percent (%)
1	Water	Blue	55202405.07	55.20240507	1.933696
2	Vegetation	Green	620664302.5	620.6643025	21.741373
3	Shallow water	Red	1143940507	1143.940507	40.071319
4	Alluvial soil	Magenta	491216407.4	491.2164074	17.206917
5	Open Land	Yellow	543737706.3	543.7377063	19.046696
	Total		2854761300	2854.7613	100

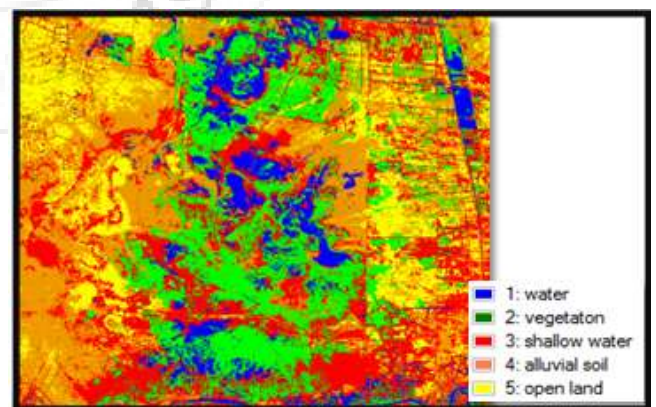


Figure 7: Classification results of supervised SVM technique for AL-Chabaish satellite image for year 2015

Table 3: Statistical results of supervised SVM Classification for AL-Chabaish Satellite Image for year 2015

Class No.	Class Name Landsat-8 (OLI) (2015)	Class Color	Class Area (m ²)	Class Area (km ²)	Percent (%)
1	Water	Blue	240919186.9	240.9191869	8.439206
2	Vegetation	Green	607130107.6	607.1301076	21.267281
3	Shallow water	Red	823857305	823.857305	28.859061
4	Alluvial soil	Magenta	701072108.8	701.0721088	24.557994
5	Open Land	Yellow	481782591.8	481.7825918	16.876458
	Total		2854761300	2854.7613	100

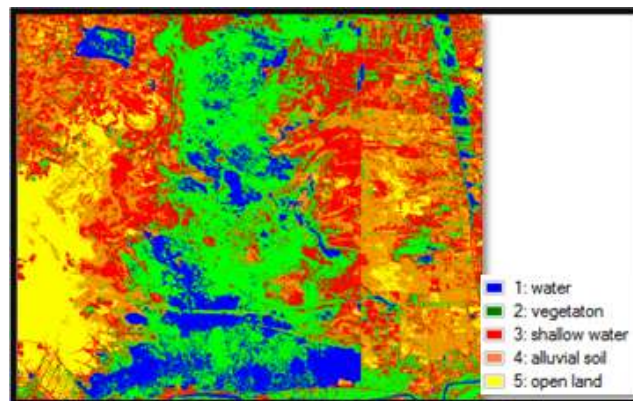


Figure 8: Classification results of supervised SVM technique for AL-Chabaish satellite image for year 2017

Table 4: Statistical results of supervised SVM Classification for AL-Chabaish Satellite Image for year 2017

Classes	1990	2000	2015	2017	change between 1990and 2000	change between 1990and 2015	change between 1990and 2017	change between 2000and 2017
Water	263.46	55.20	240.92	335.00	-208.25	-22.54	-71.54	279.80
Vegetation	1239.14	620.66	607.13	869.80	-618.47	-632.01	369.34	249.14
shallow water	620.89	1143.94	823.86	719.05	523.05	202.97	-98.16	-424.89
alluvial soil	427.44	491.22	701.07	595.13	63.77	273.63	-167.68	103.91
open land	303.84	543.74	481.78	335.79	239.90	177.95	-31.95	-207.95

Table 5: The change in the years 2000, 2015, and 2017 comparing with 1990 using supervised SVM technique

Class No.	Class Name Landsat-8 (OLI) (2017)	Class Color	Class Area (m ²)	Class Area (km ²)	Percent (%)
1	Water	Blue	335000700.3	335.0007003	11.734806
2	Vegetation	Green	869800491.6	869.8004916	30.468414
3	Shallow water	Red	719046913.5	719.0469135	25.187637
4	Alluvial soil	Magenta	595125008.4	595.1250084	20.846752
5	Open Land	Yellow	335788186.2	335.7881862	11.762391
	Total		2854761300	2854.7613	100

3.5 Classification Accuracy

In this work, to estimate the accuracy of classification, using the information collected during the field view and number of random points which chosen area for different bands of the study area which are represented as a classification map to be compared with the classification results by means the parameters, these parameters represent the total accuracy, user's accuracy, and producer accuracy respectively, which can be represented mathematically by the following empirical relations: then compared with the classification results. In this work, the accuracy assessment was done for supervised SVM classification technique with MATLAB software for years 1990, 2000, 2015, and 2017. Tables (6-9) present error matrix with producers, users, and overall accuracy calculations for years 1991, 2000, 2015, and 2017, respectively.

Table 6: error matrix with producers, users, and overall accuracy calculations for supervised SVM classification technique for AL-Chabaish marshes satellite image Landsat5-TM (1990)

Classes	water	vegetation	shallow water	alluvial soil	open land	total Pixels	user's accuracy
Water	19176	235	0	0	0	19411	98.7893
Vegetation	1134	19426	1127	0	0	21687	89.5744
shallow water	23	1233	14146	1857	24	17283	81.8492
alluvial soil	0	0	177	16185	744	17106	94.6159
open land	0	0	0	1102	8267	9369	88.2378
total Pixels	20333	20894	15450	19144	9035	84856	
Producer's Accuracy	94.31%	92.97%	91.56%	84.54%	91.50%		
overall accuracy	90.98%						

Table 7: error matrix with producers, users, and overall accuracy calculations for supervised SVM classification technique for AL-Chabaish marshes satellite image Landsat5-TM 2000

Classes	Water	vegetation	shallow water	alluvial soil	open land	total Pixels	user's accuracy
Water	2346	11	0	0	0	2357	99.5333
vegetation	102	2313	0	0	0	2415	95.7764
shallow water	11	115	1878	127	23	2154	87.1866
alluvial soil	0	14	155	3417	121	3707	92.177
open land	0	0	30	212	2393	2635	90.8159
total Pixels	2459	2453	2063	3756	2537	13268	
Producer's Accuracy	95.40%	94.29%	91.03%	90.97%	94.32%		
overall accuracy	93.21%						

Table 8: Error matrix with producers, users, and overall accuracy calculations for supervised SVM classification technique for AL-Chabaish marshes satellite image Landsat5-TM 2015

Classes	Water	vegetation	shallow water	alluvial soil	open land	total Pixels	user's accuracy
Water	2299	367	0	1	0	2667	86.2017
Vegetation	125	3655	344	0	0	4124	88.6275
shallow water	45	0	5136	87	0	5268	97.4943
alluvial soil	0	0	232	1296	55	1583	81.8699
open land	0	0	0	28	1078	1106	97.4684
total Pixels	2469	4022	5712	1412	1133	14748	
Producer's Accuracy	93.11%	90.88%	89.92%	91.78%	95.15%		
overall accuracy	92.17%						

Table 9: error matrix with producers, users, and overall accuracy calculations for supervised SVM classification technique for AL-Chabaish marshes satellite image Landsat5-TM 2017

Classes	Water	Vegetation	shallow water	alluvial soil	open land	total Pixels	user's accuracy
Water	1987	95	0	0	0	2082	95.4371
Vegetation	75	3466	99	0	0	3640	95.2198
shallow water	0	102	2830	95	63	3090	91.5858
alluvial soil	0	0	50	1130	87	1267	89.1871
open land	0	0	67	17	905	989	91.5066
total Pixels	2062	3663	3046	1242	1055	11068	
Producer's Accuracy	96.36%	94.62%	92.91%	90.98%	85.78%		
overall accuracy	92.13%						

3.6 Satellite Image Classification using ENVI 5.3 Software:

In this section, we utilized, supervised (maximum likelihood) using ENVI 5.3 software programming 2017 to classification Landsat TM, ETM+ and OLI satellite images of AL-Chabaish marshes for years 1990, 2000, 2015 and 2017. The application of the supervisory classification method requires a multi-spectral image consisting of two or more domains. Also know ahead of time the characteristics of the geographical area covered by the image to be classified in order to determine the number of classification categories and to select training areas. Training areas are image locations that are selected to represent the spectra of geo-specific phenomena in the area covered by the image. Therefore, the first step in this method is to limit and identify types. The geographical phenomena in the area covered by the image are done either on the field or using modern maps available. The image to be selected on the screen to select and plot the training zones representing each type of geospatial. Each category of classification must be drawn on the screen image. An appropriate number of image cells representing the training areas are not concentrated in part but will be distributed throughout the entire image, number of the training data illustrate in table 10. By drawing the boundaries of the training areas in the image, the computer recognizes the values of the image range cells for each of the specific classification categories to be relied upon in the classification process. In this section, we applied supervised Maximum Likelihood classification method on AL-Chabaish marshes satellite images for years 1990, 2000, 2015, 2017 as shown in figures (9- 12) respectively. Tables (11- 14) presents the statistical result of this classification methods for years 1990, 2000, 2015 and 2017 respectively, Table 15 illustrated the change in years 2000, 2015 and 2017 comparing with year 1990, ,

Table 10: The Number of Pixels Selected as Training Area for Each Class in Each Satellite Image using supervised (maximum likelihood) classification method

Class No.	Class Name	(TM) Images 1990	(ETM+) Images 2000	(OLI) Images 2015	(OLI) Images 2017
1	Water	146	143	138	153
2	Vegetation	141	153	144	127
3	Shallow water	140	142	139	169
4	Alluvial soil	148	173	144	124
5	Open Land	115	148	187	113
	Total	690	759	752	686

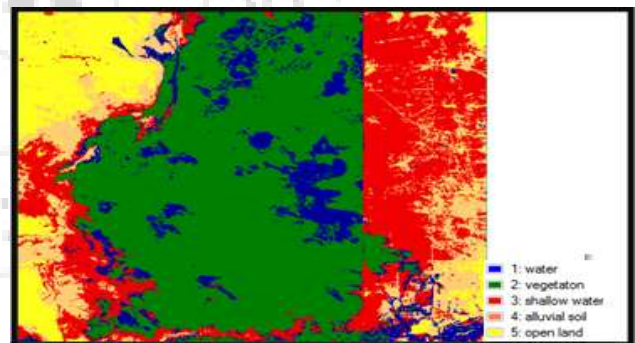


Figure 9: Classification results of supervised Maximum Likelihood technique for AL-Chabaish satellite image for year 1990.

Table 11: Statistical results of supervised Maximum Likelihood Classification for AL-Chabaish Satellite Image for year 1990

Class No.	Class Name Landsat-8 (OLI) (1990)	Class Color	Class Area (m ²)	Class Area (km ²)	Percent (%)
1	Water	Blue	293364000	293.364	10.276306
2	Vegetation	Green	1224399600	1224.3996	42.889737
3	Shallow water	Red	674100900	674.1009	23.613214
4	Alluvial soil	Magenta	352552500	352.5525	12.349631
5	Open Land	Yellow	310344300	310.3443	10.871112
	Total		2854761300	2854.7613	100

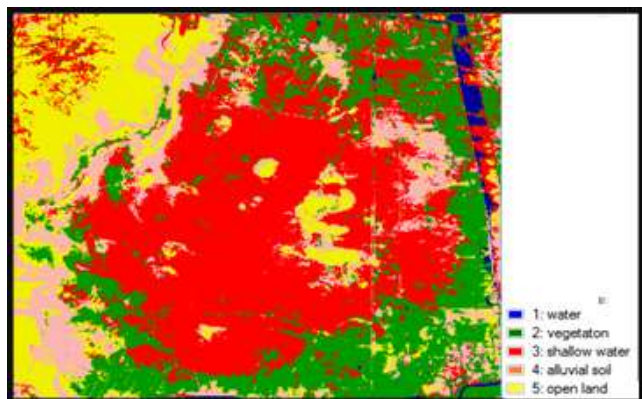


Figure 10: Classification results of supervised Maximum Likelihood technique for AL-Chabaish satellite image for year 2000

Table 12: Statistical results of supervised Maximum Likelihood Classification for AL-Chabaish Satellite Image for year 2000

Class No.	Class Name Landsat-8 (OLI) (2000)	Class Color	Class Area (m ²)	Class Area (km ²)	Percent (%)
1	Water	Blue	48683700	48.6837	1.705351
2	Vegetation	Green	685507500	685.5075	24.012778
3	Shallow water	Red	1172671200	1172.6712	41.077732
4	Alluvial soil	Magenta	437852700	437.8527	15.337629
5	Open Land	Yellow	510046200	510.0462	17.86651
	Total		2854761300	2854.7613	100

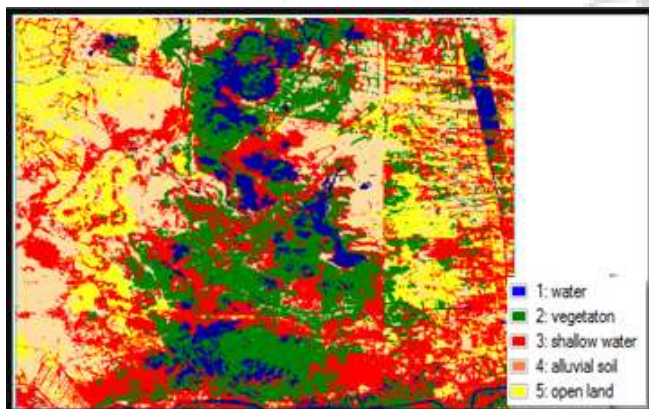


Figure 11: classification results of supervised Maximum Likelihood technique for AL-Chabaish satellite image for year 2015.

Table 15: The change in the years 2000, 2015, and 2017 comparing with 1990 using supervised Maximum Likelihood method

Classes	1990	2000	2015	2017	change between 1990 and 2000	change between 1990 and 2015	change between 2000 and 2015	change between 1990 and 2017
Water	293.36	48.68	213.93	303.94	-244.68	-79.43	-10.58	255.26
vegetation	1224.40	685.51	652.75	871.71	-538.89	-571.65	352.69	186.21
shallow water	674.10	1172.67	881.49	839.04	498.57	207.39	-164.94	-333.63
alluvial soil	352.55	437.85	656.11	550.47	85.30	303.56	-197.92	112.62
open land	310.34	510.05	450.48	289.59	199.70	140.14	20.76	-220.46

4. Field Visit

During this work, areas appeared unclassified with five classes in addition there was a small area appeared with high temperature so it was necessary to visit the marshland and this is what happened on the 17 January 2018. During this visit coordinates of different sites were recorded using a

Table 13: Statistical results of supervised Maximum Likelihood Classification for AL-Chabaish Satellite Image for year 2015

Class No.	Class Name Landsat-8 (OLI) (2015)	Class Color	Class Area (m ²)	Class Area (km ²)	Percent (%)
1	Water	Blue	213932700	213.9327	7.493891
2	Vegetation	Green	652750200	652.7502	22.865316
3	Shallow water	Red	881487900	881.4879	30.877815
4	Alluvial soil	Magenta	656109000	656.109	22.982972
5	Open Land	Yellow	450481500	450.4815	15.780006
	Total		2854761300	2854.7613	100

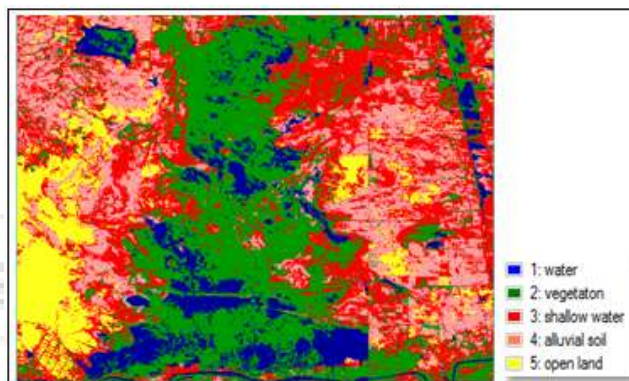


Figure 12: Classification results of supervised Maximum Likelihood technique for AL-Chabaish satellite image for year 2017

Table 14: Statistical results of supervised Maximum Likelihood Classification for AL-Chabaish Satellite Image for year 2017

Class No.	Class Name Landsat-8 (OLI) (2017)	Class Color	Class Area (m ²)	Class Area (km ²)	Percent (%)
1	Water	Blue	303944400	303.9444	10.646929
2	Vegetation	Green	871713000	871.713	30.535408
3	Shallow water	Red	839043900	839.0439	29.391035
4	Alluvial soil	Magenta	550471500	550.4715	19.282575
5	Open Land	Yellow	289588500	289.5885	10.144053
	Total		2854761300	2854.7613	100

Global Position System (GPS) which was used to verify the training site (water, vegetation, Shallow water, alluvial soil, openland). During this visit the following information had been collected:

- 1) Gathering information about a number of classes as well as knowing the environmental change taking place in the region.

2) Collection of information about each class such as, water, soil, vegetation and other classes, as well as taking photos and collecting GPS coordinates.

[7] Marshes property in the world heritage <https://iraqi-marshlands.mowr.gov.iq>.

[8] T. A. Moughal (2013) **"Hyperspectral image classification using Support Vector Machine"**. Journal of Physics: Conference Series **439** 012042.

5. Conclusions

Results of this work leads to several important conclusions, including:

- 1) The results from applying Support Vectors Machine (SVM) classification method for AL-Chabaish marshes show that marsh vegetation and water decreased about 49.88%, 78.95%, respectively. While openland, alluvial soil and shallow water increase about 78.96%, 14.92% and 84.24%, respectively in 2000 compares with 1990, after drying the marshes. While the results after starting to fill the marshes show that vegetation, water and alluvial soil increase about 28.09%, 83.29% and 17.46% respectively. While openland and shallow water decreased about 61.93% and 59.09% respectively in 2017 compares with 2000.
- 2) The results of the proposed method approximately similar to the results from applying supervised (Maximum likelihood) Classification method.
- 3) Two supervised classification methods were used but the results of the proposed method proved its superiority because the classification accuracy is 90.98 %, 93.21%, 92.17% and 92.13% for years 1990, 2000, 2015 and 2017 respectively.
- 4) The environmental changes was very clear in Al Chabaish marshes during the period 1990- 2017, the results indicate a decrease in vegetation and water with the increase in the openland, alluvial soils and shallow water.
- 5) The results from applying Support Vectors Machine (SVM) marshes) are agreement with field visit to the study area in (17 January 2018), where the classification accuracy is 92.34%.

References

- [1] Riadh K.A., (2005)'Change Detection of Environmental system Using satellite images in Shatt AL-Arab region", M.SC. Thesis, University of Technology, Iraq.
- [2] Daptardar A. A. and Vishal J. K., 2013" Introduction to Remote Sensors and Image Processing and its Applications ", International Journal of Latest Trends in Engineering and Technology (IJLTET), vol. 1, IDEAS-, ISSN: 2278-621X.
- [3] James, B. C. and Randolph, H. W., 2011" Introduction to Remote sensing", Fifth Edition, The Guilford Press, New York , London, .
- [4] Gustavo, C. , Gustavo C., Devis T., Luis G., Sandra J., and Jesús M., 2011"Remote Sensing Image Processing", Fourth editor, University of Texas, Austin, .
- [5] N. Mechat, N. Saadia, N.K. M'Sirdi, N. Djelal, 2012 **"Lane detection and tracking by monocular vision system in road vehicle"**, Image and Signal Processing (CISP) 2012 5th International Congress on, pp. 1276-1282,
- [6] Dwi Ratna, Budi Setyono, Tyara Herdha. (2016) **"Bullet Image Classification using Support Vector Machine (SVM)"**, Journal of Physics: Conference Series 693 012009.

Volume 7 Issue 6, June 2018

www.ijsr.net

[Licensed Under Creative Commons Attribution CC BY](https://creativecommons.org/licenses/by/4.0/)